

## Aeroacoustical Study of the Serrated Ventilation Dampers

Joanna Maria KOPANIA<sup>1</sup> , Grzegorz BOGUSŁAWSKI<sup>2</sup> , Kamil WÓJCIAK<sup>3</sup> , Patryk GAJ<sup>4</sup> 

<sup>1,2</sup> Lodz University of Technology, Żeromskiego 116, 90-924 Lodz, Poland

<sup>3,4</sup> Institute of Power Engineering, Mory 8, 01-330 Warsaw, Poland

**Corresponding author:** Joanna Maria KOPANIA, email: joanna.kopania@p.lodz.pl

**Abstract** The serrated ventilation dampers for regulation of airflow volume were tested. The computer fluid flow analysis was conducted using the Comsol program. The nature of the flow through the serrated ventilation damper was analyzed to identify the different turbulence regions formed on the airflow field. Additionally, the aerodynamical and acoustical parameters of these blades of ventilation dampers with different serrated trailing and/or leading-edge were studied. The aeroacoustic studies were done in the reverberation room. The sound power level and loss coefficient were determined for the studied models.

**Keywords:** aeroacoustic, ventilation, plane damper, serrated edge.

### 1. Introduction

Maintaining air quality in buildings is essential to the functions of our everyday. HVAC systems are necessary to keep indoor spaces warm, cool, and full of high-quality and clean air and it is used in many industrial and residential spaces. During the designing of a new building or rebuilding the older one, the design of ventilation or climatization systems (HVAC) is taken into account, especially the ventilation rate, airflow direction, air distribution or air pattern flow [1-3]. This is connected with the appropriate selection of some elements of the system like fans, ducts, tubes, angles, filters, air valves, silencers, diffusers, exhaust elements – grid. These elements are also sources of noise in the ventilation system. General, there are two main paths for noise generation in HVAC systems [4, 5]:

- acoustic energy can propagate through the duct airspace (airborne) – is mostly due to fan or flow noise, for example, turbulence or vortex shedding caused by flow over a cavity or sharp edge or obstacle in fluid flow. Airborne noise propagates through the duct airspace to the rooms. Airborne noise is typically reduced by using sound-absorbing material like fibre or foam, adding silencers or plenums, or extending the length of the ducts.
- through the duct structure (structure-borne) itself – is propagated through ductwork, piping, and mounts and transmitted to other parts of the building. Sound is radiated from vibrating walls, floors and ceilings. Additionally, sound can be radiated from the ductwork or plenum itself. This is typically referred to as breakout noise. The structure-borne noise in the duct system can be attenuated by using proper isolation or adding additional damping to the structure.

There is an interplay between acoustics and the primary function of HVAC devices which consists in providing a proper quantity of well-mixed air to the building occupants but with respect to their acoustic comfort. The increasing popularity of the energy efficiency and acoustics comfort of the HVAC systems are the Building energy efficiency tendencies in Europe, like the Energy Performance of Buildings Directive (EPBD) recast [6] and the Ecodesign requirements for ventilation units [7]. The noise-sensitive of all HVAC products is the "air terminals" with flow regulations elements (CAV or VAV dampers) because they are always mounted in or directly over occupied spaces. As these two elements are the final components in many built-up air delivery systems and those closest to the building occupants, both are critical components in the acoustical design of a space.

In this work, the aeroacoustics parameters of damper used in HVAC systems were studied for a different construction of damper's plates. The construction of the damper's plates was based on the solution used in nature, like the owl's wings. The silent flight of owls results from three special characteristics: the serrated leading edge, the fringe on the trailing feathers, and the velvet-like surface. Two main species of owl – nocturnal – "good hearing" and diurnal – "good seeing" are known in the biology of these birds. The leading edge of diurnal owls have small arcs but the leading edge of the nocturnal owls have teeth. The new construction of damper's plates with modified edges was studied in this work, as teeth and as arcs. Comsol was used to analyze the nine damper's plate designs – one based

without the modified edges and eight with modified edges. CFD analyses were performed in order to see flow velocity inside and pressure drop. The next step was the experimental measurements in the reverberation room according to ISO 5135 [8]. The sound noise power  $L_w$  of the studied units and pressure dropped were determined.

## 2. CFD analysis

For CFD simulation 3D solid models of the damper's plate were created by the Inventor program. Plate angle can be easily changed by using this program and changing plate angle is also essential to this study. In Figure 1 simplified example of the damper's plate geometry is given with the characteristic parameters of serration ( $h$  and  $d$ ).

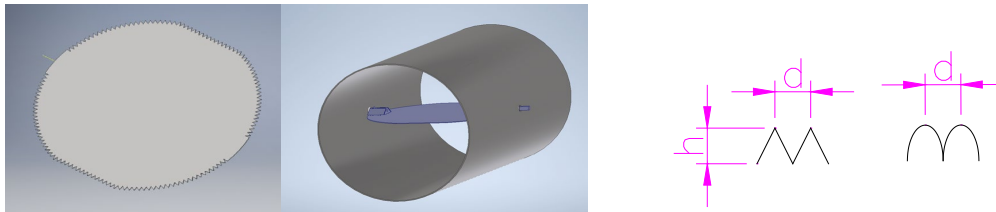


**Figure 1.** The example model of the tested damper (on the left) and its connection to the duct (in the middle) and the parameters of serrations (on the right).

After drawing simplified geometry, extraction of fluid volume is needed to perform CFD analysis in Comsol [9], so the inverted models were created in Inventor. Analyzed units had 246 mm outer diameter. The plate of dampers had a thickness of 1 mm. The diameter of the housing was 250 mm and it was the fluid domain. In reality, the whole length of the units was 800 mm. This length is divided as inlet – 200 mm from the axis of the damper; outlet – 600 mm from the axis of the damper. Two positions of dampers:  $0^\circ$  (100% opened) and  $45^\circ$  were studied. The nine test objects are used in CFD analyses. All dimensions of the tested dampers are listed in Table 1.

**Table 1.** Characteristic parameters of the tested dampers in millimetres.

VARIANT	EDGE	SHAPE	$h$	$d$
"base"	-	-	-	-
1	trailing	teeth	5	5
2	trailing	arches	5	5
3	trailing	teeth	10	5
4	trailing	arches	10	5
5	trailing+leading	teeth	5	5
6	trailing+leading	arches	5	5
7	trailing+leading	teeth	10	5
8	trailing+leading	arches	10	5

Most physics interfaces within COMSOL Multiphysics use the finite element method to solve the underlying partial differential equations. Finite element methods are widely used by the numerical analysis community to study numerical methods for fluid flow there is no theoretical or practical support for the hypothesis that finite volume methods are superior to finite element methods for fluid flow. So, we used the Comsol programme in our work. The mesh is composed of tetrahedral elements. In Comsol programme mesh elements were physic-controlled with size fine. The numbers of elements for the damper's plate in position:  $0^\circ$  – 350694; at an angle of  $45^\circ$  – 289162 were obtained. In order to reduce computational times, investigations were made in half of the damper system and a symmetric plane boundary condition is used. Three-dimensional calculations were made as a stationary analysis. The standard SST model is selected for the turbulence evaluation with an intensity of 5%, solution condition tolerance of 0.001, and solves GMRES 50 iteration. The material was the air with a constant temperature, density  $1.2 \text{ kg/m}^3$  and a viscosity of  $18.053\text{e-}6 \text{ Pa}\cdot\text{s}$ . Three inlet velocities were simulated: 2 m/s; 6 m/s and 12 m/s. The velocity vector at the ventilation duct inlet has the same value throughout the entire duct

area was established. On the outlet, the pressure condition was used ( $P_{\text{static}} = 0$  Pa). The automatic wall treatment (no slip walls condition) was chosen.

After simulation, the velocity behind the damper plane was calculated at different distances. The distances plane are shown in Figure 2 for the 0 and 45 positions of the plane, but the zero position is in the rotary axis of the damper.

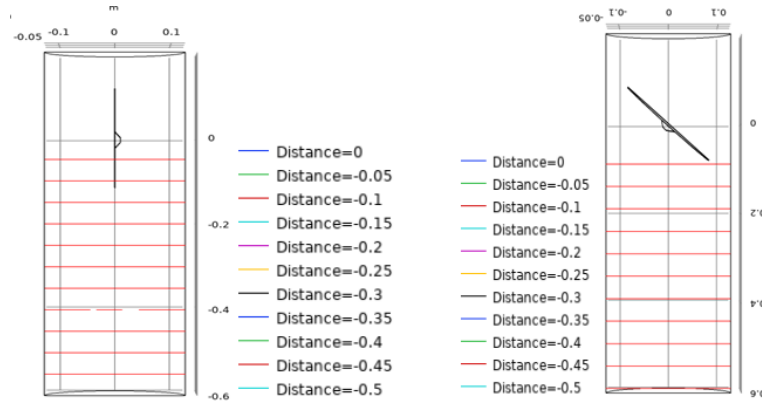


**Figure 2.** The planes of the velocity parameters read behind the damper's plate.

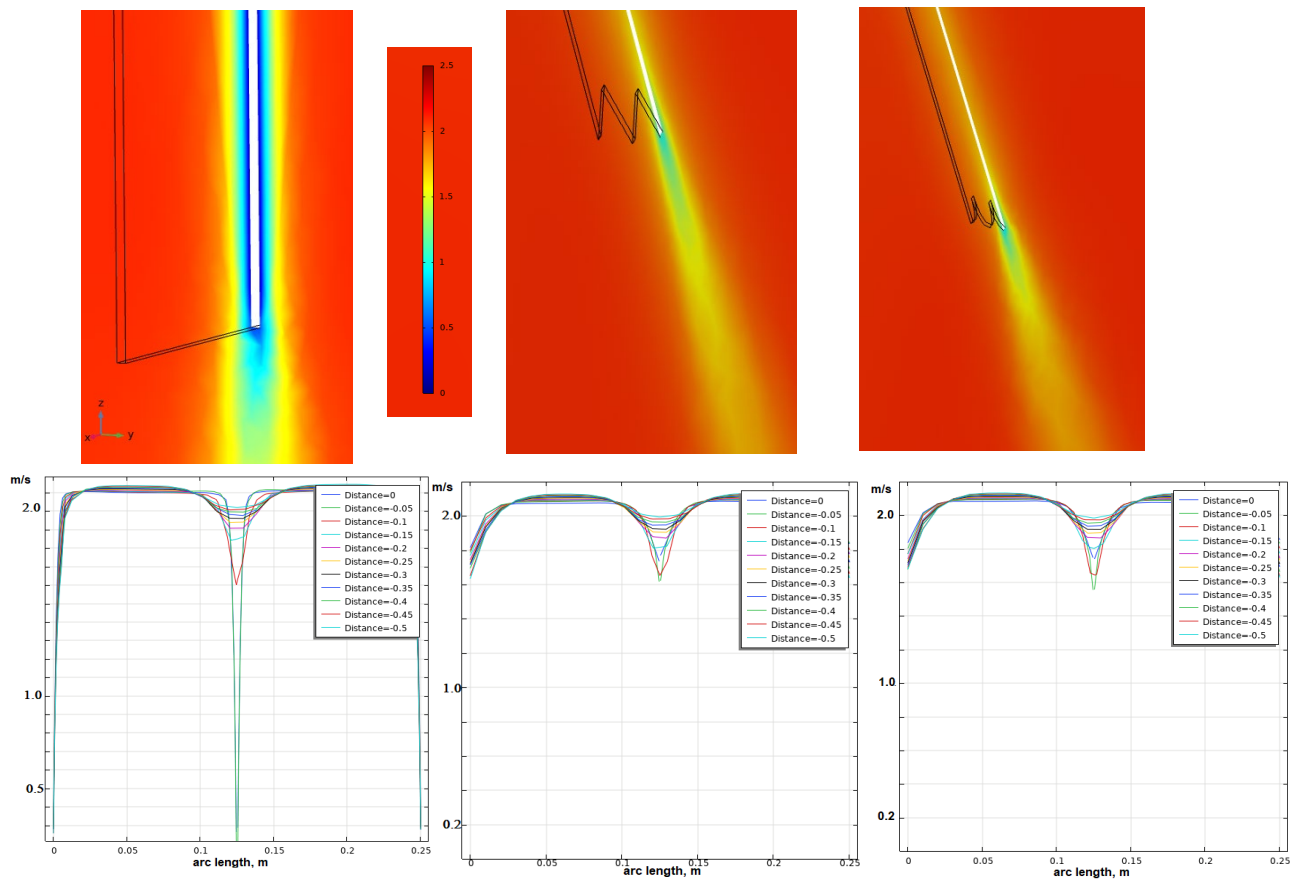
Velocity distribution for 2 m/s inlet flow, inside of the studied dampers (behind the plate) is given in Figure 3. Red colour represents higher velocity values and light blue colour represents low-velocity values. As we have seen in Figure 3 the lower velocity parameters behind the damper's plane were obtained for the damper's plane with a serrated edge. As we have seen the higher velocity parameters behind the damper's plane were obtained for the damper's plane with a serrated edge. Around the "base" damper plane (Figure 3, on the left), the lower velocity parameters are observed, as a blue field - Figure 3 upper picture. This is the stagnation point formed in the air flow field where the local velocity of air approaches zero. In the throttle flow, a stagnation point is formed near the damper's plate surface where the air is brought to rest due to sudden obstruction in flow. That means that the significant decrease of velocity takes place close to the "base" damper plate - until 0.3 m/s. For damper plate variant 3 (in the middle) and variant 4 (on the right), the velocity near the plate is around 1.5 m/s. So, the teeth and arcs on the edge impact the flow field around the damper's plate and we can conclude, that for these ones the equalization of the flow parameters is faster than for the "base" plate. It can be seen also in Figure 3 bottom picture, where the velocities profiles behind the studied damper's planes are drawn. As can be seen from Figure 4, the velocity of the 45° damper's plane opening positions indicates the eddy current of the airflow. It is observed from the streamlines the generation of vortices that move in the direction behind the damper's plane because of the high disturbance of the flow. The wake region containing the vortices is created downstream of the damper's plate (on the left side of each picture). This wake region decays by moving inside the fluid domain in the outlet direction. The streamlines become uniform which indicates the reduction of the flow disturbance. As we can see in Figure 4 the lower velocity near the duct wall is observed for serrated (variant 7) and arcs (variant 8) damper's plane than for the "base" one at the characteristic points marked by the vertical and horizontal lines.

Table 2 lists the pressure drops ( $\Delta P$ ) of the simulated flow damper's plane. All numbers are the average results from the inlet of the flow domain ( $P_1$ ) and its outlet ( $P_2$ ) according to the formula [10]:

$$\Delta P = P_1 - P_2 = (8\mu L v_{\text{avg}}) / R^2, \quad (1)$$

where  $\mu$  is dynamic viscosity,  $L$  is the length of pipe,  $v_{\text{avg}}$  is the average velocity,  $R$  is the pipe radius.

The pressure drops calculated range from 29.4 Pa to 1040.9 Pa for the "base" damper plate. The "base" damper plate yielded a higher pressure drop than serrated and arcs plates. The lower pressure drops were calculated for variants 3, 5, 7 and 8 of the damper's plate. The simulation results also showed that the effect of the flow on the velocity profile was highly dependent on the location of the measurement plane behind the damper's plane.



**Figure 3.** The velocity parameters for 2 m/s inlet flow around the dampers blade: on the left – “base”; in the middle – variant 3; on the right – variant 4. Damper’s planes are in 0° position – fully opened.

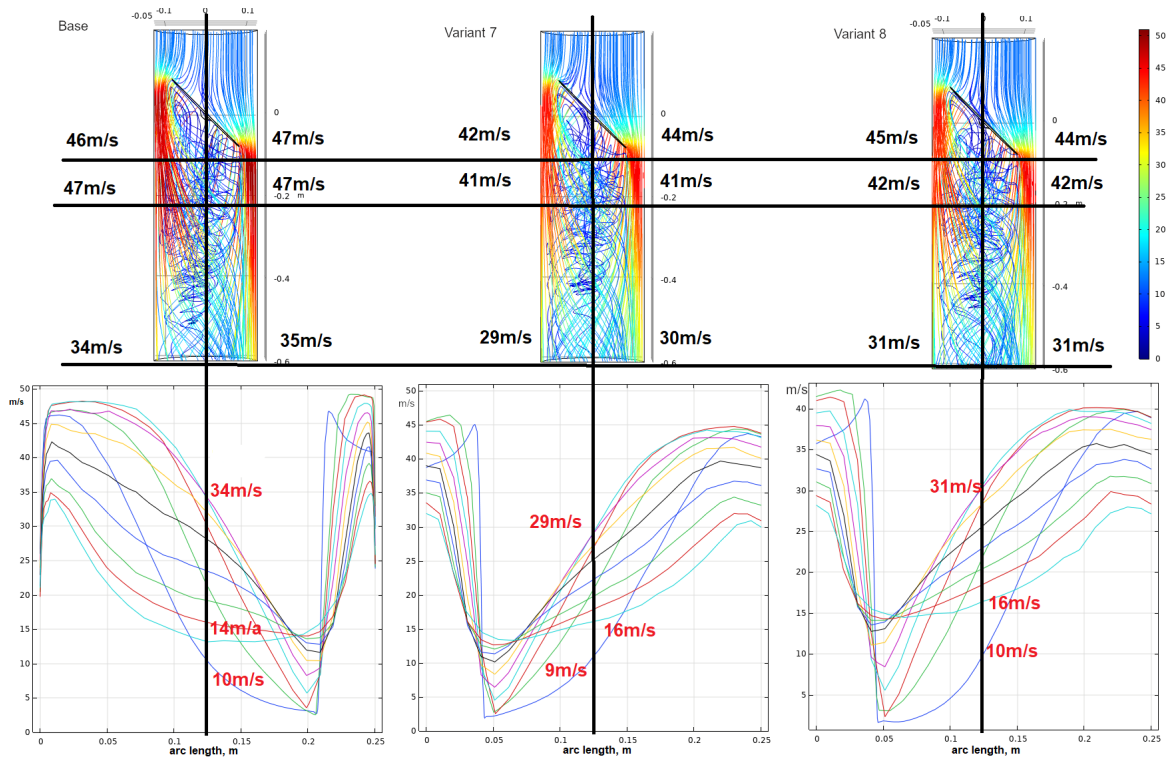


**Figure 4.** The velocity streamlines for 12 m/s inlet flow around the dampers blade: on the left – “base”; in the middle – variant 7; on the right – variant 8. Damper’s planes are in 45° position.

**Table 2.** The pressure drop between the inlet and outlet plane of the domain for studied models of the damper's plane.

Velocity m/s	$\Delta P$ - pressure drop, Pa								
	"base"	1	2	3	4	5	6	7	8
2	29.4	26.0	27.2	23.6	25.8	24.2	26.3	23.6	23.8
6	261.4	230.7	242.0	209.7	228.9	215.0	234.4	181.0	210.7
12	1040.9	919.8	966.1	837.5	914.8	857.6	934.7	723.3	842.3

The simulation results showed that the best design, in terms of reducing pressure loss, was the variants 3, 5, 7 and 8 of plates, and they were selected as the prototypes to be evaluated in the laboratory test. In order to compare with them, the "base" damper plate and variant 1 of the plate were also used in the real test.

### 3. Measurement and results

The measurements were made on a test stand built following the norm ISO 5135:2020: Acoustics — Determination of sound power levels of noise from air-terminal devices, air-terminal units, dampers and valves by measurement in a reverberation test room with a volume of 237.0 m<sup>3</sup> and an area of 231.5 m<sup>2</sup> and with non-parallel walls. The tested object was connected to the centrifugal fan through three absorption silencers and a noise source outside the chamber as shown in Figure 5.

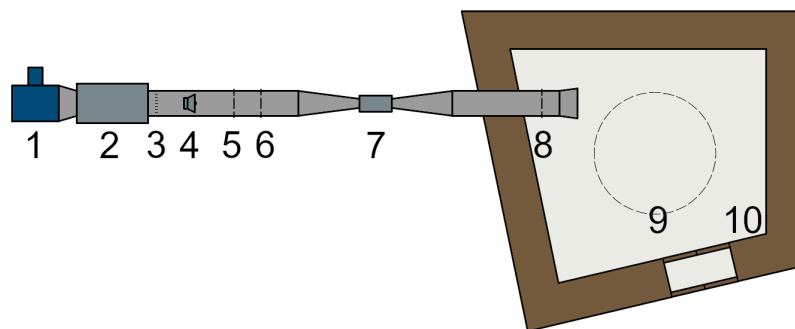


**Figure 5.** Test stand with reverberation room scheme: 1 – fan, 2 – set of three silencers, 3 – flow straightener, 4 – noise source, 5 – pressure and temperature measurement, 6 – flow velocity measurement, 7 – test object, 8 – pressure measurement, 9 – microphone path, 10 – reverberation room.

The tests were carried out with the pink noise source turned on for four flow velocities of 2, 6 and 12 m/s at the inlet of the tested object. The volumetric flow was set by changing the rotation frequency of the fan motor. For this purpose, a three-phase inverter was connected to the motor. Flow velocity was measured using the Prandtl Tube. The static pressure drop on the tested dampers was measured through and behind the unit at four evenly located points around the channel according to PN EN ISO 1751 "Ventilation for buildings – air terminal devices – aerodynamic testing of damper and valves" [11].

The generated noise is determined by sound power level, measured and calculated under PN-EN ISO 3741:2011 "Acoustics – Determination of sound power levels and acoustic energy levels of noise sources based on sound pressure measurements – Precision methods in reverberation chambers" [12]. The Brüel&Kjær 2144 measuring set with the Brüel&Kjær 3923 rotary table was used for the measurements. The sound pressure was measured at nine points in a circle with a radius of 1.7 m (circumference of 10.7 m). Measured in 1/3 octaves in the range from 100 Hz to 10 000 Hz. The measurement time is set to 30 s. Background noise was measured for a stand without flow to determine the background correction  $K_1$ . Reverberation was measured for four omnidirectional loudspeaker settings with three microphone settings and four speaker positions. Before and after all measurements were made, the background level was measured and calibrated using the Brüel&Kjær 4231 calibrator. After measuring each setting, the temperature, relative humidity and atmospheric pressure necessary for calculating the sound power were recorded.

The ISO 1751 standard gives guidelines the calculating the aerodynamic parameters of dampers. The coefficient  $C_D$  and loss coefficient  $\xi$  were calculated and given in Table 3. The low values of loss coefficient  $\xi$  for variants 3, 5 and 8 were obtained at  $0^\circ$  angle. But at  $45^\circ$  angle the low values were for variants 5 and 7. In Figure 6 pressure measurement results for the studied variants of damper's plate at  $45^\circ$  angle opening are given in pressure drop versus flow volume. As seen in the figure the lowest pressure drop for variant 5 is observed. For fully opening the damper's plate pressure is negative, which means the plate is parallel with the flow (the graph is not included)

The differences between the 1/3-octave level of sound power of the "base" damper and studied variants of the damper's plate (without the A-correction) were used to present the results of noise reduction ( $\Delta L_w$ ), using the equation (2).

$$\Delta L_w = L_w^{\text{"base"}} - L_w^{\text{"variant"}} \quad (2)$$

where  $L_w^{\text{"base"}}$  – the level of the sound power in the frequency band considered for the "base" damper plate,  $L_w^{\text{"variant"}}$  – the level of the sound power in the frequency band considered for the studied variant of damper plate. Because the sound power level does not depend on the airflow velocity, average values are used in the calculations. The example graphs for  $45^\circ$  angle position of damper's plate are presented in Figures 7 and 8. For all studied variants of damper's plate with edge modifications, the noise reduction in this position of the plate was observed, which is evidenced by positive values of 1/3-octave differential spectrum in Figures 7 and 8. However, variant 3 is an exception below 4 kHz, where the 1/3-octave differential spectrum has negative values.

**Table 3.** The  $C_D$  coefficient and loss coefficient  $\xi$  of studied damper's plate at  $0^\circ$  and  $45^\circ$  angle positions.

Variant	$0^\circ$		$45^\circ$	
	$C_D$	$\xi$	$C_D$	$\xi$
"base"	2.20	0.21	0.30	11.10
1	2.13	0.12	0.27	14.00
3	5.23	0.04	0.28	12.60
5	3.55	0.08	0.33	9.30
7	2.26	0.20	0.31	10.60
8	4.43	0.05	0.29	11.60

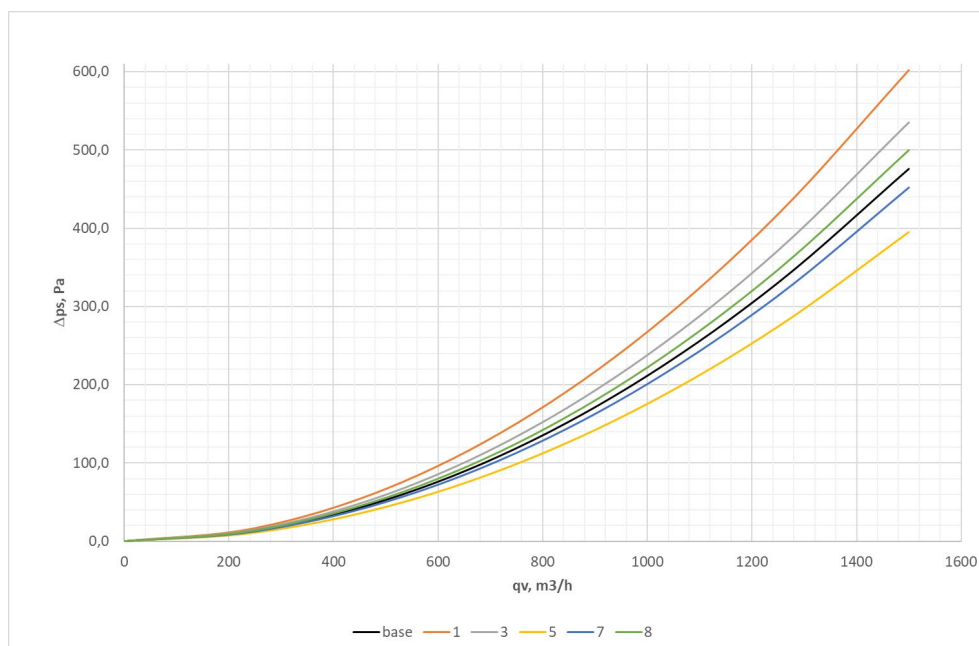


**Figure 6.** The pressure drop for "base", variant 1, variant 3, variant 5, variant 7 and variant 8 of the damper's plane at  $45^\circ$  opening angle.

The sound power level with A corrections for the studied damper's plate is presented in Table 4. As can be seen, at a fully opened position there are no significant differences between the "base" damper and the studied variants. The maximum difference is 1,5 dB for variant 1 at 1060 m/h and 1415 m/h. But it could be assumed that it is in with the margin of some error resulting from inaccurate measurement technics (the uncertainty of the measurements according to the PN EN ISO 5135 and PN EN ISO 3741 will be the subject of another work). But in the second case, when the studied damper's plates are in 45° position, the 4.5 dB lower  $L_{WA}$  values for the variant 5 of damper's plate at 705 m/h were obtained and properly 3.8 dB and 3.2 dB in higher flow volume. At this flow volume, the noise reduction was observed also for variants 1 and 8 studied dampers. But at higher flow volume the trend is disappeared.

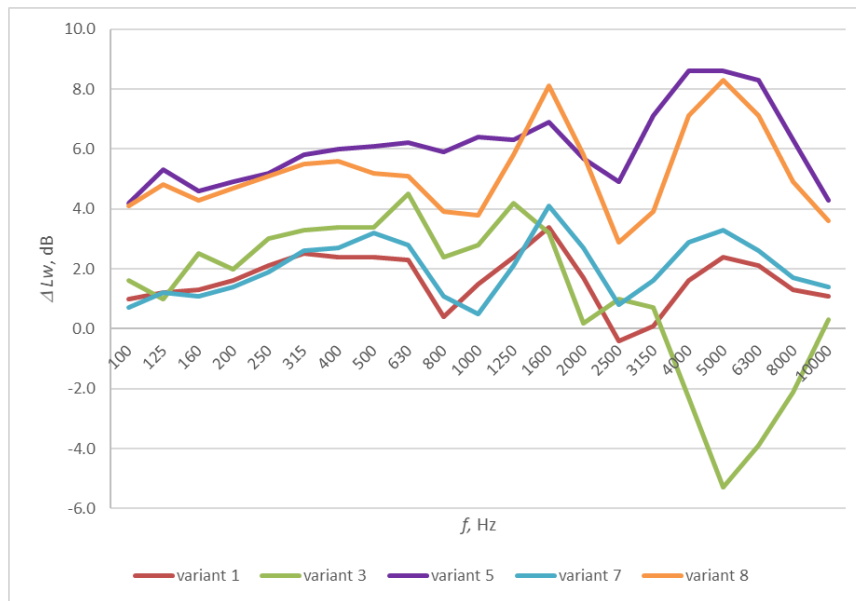


**Figure 7.** 1/3-octave differential spectrum between “base” damper and studied variants damper’s plate at 705 m<sup>3</sup>/h, for 45° angle position.

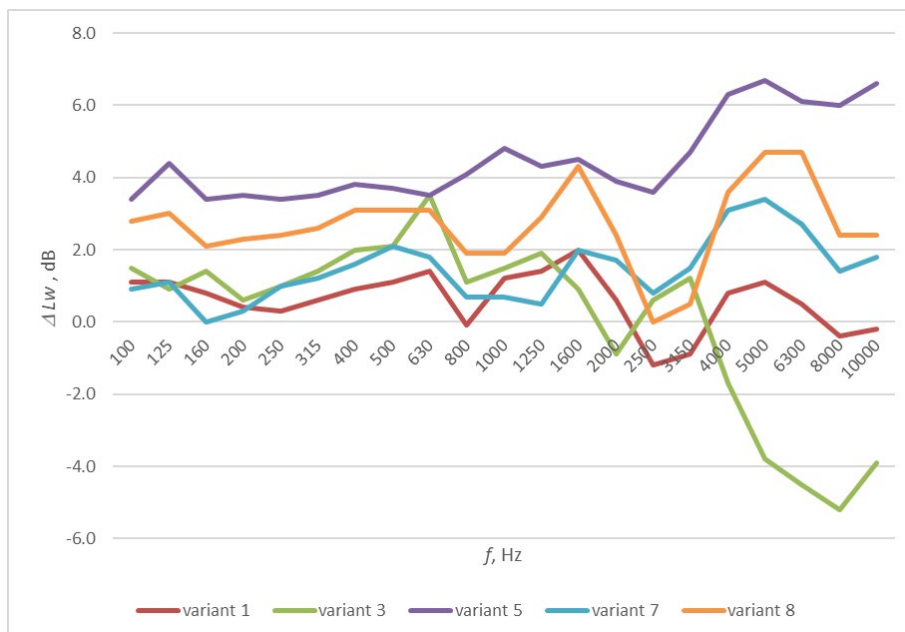


**Figure 8.** 1/3-octave differential spectrum between “base” damper and studied variants damper’s plate at 1060 m<sup>3</sup>/h, for 45° angle position.

**Table 4.** The sound power level  $L_{wA}$  for the studied variant of damper's plate in different flow volumes and angle positions.

Variant	$Q_v, \text{m}^3/\text{h}$					
	705	1060	1415	705	1060	1415
	$L_{wA}$ for $0^\circ$ , dB			$L_{wA}$ for $45^\circ$ , dB		
"base"	27.8	38.5	46.8	52.0	62.0	69.2
1	27.7	37.0	45.3	50.4	61.6	69.2
3	26.7	36.4	45.2	50.3	61.5	69.4
5	27.3	37.8	46.2	45.8	57.7	66.2
7	27.2	38.6	46.9	49.9	60.6	67.1
8	27.0	37.9	46.0	47.0	59.9	68.5

According to early published papers about the serrated leading edge, serration contributes to flow stabilization and can prevent the laminar separation of flow on the damper's plane surface. The serrations of the leading edge behave as a set of closely streamwise vortex generators and can reduce the flow separation and boundary layer thickness, and also stabilize the airflow on the damper surface which is connected with the noise of the unit.

## 5. Conclusions

- The velocity field over different cross-sections of the damper's plate with and without edges modifications was analysed. The study of velocity parameters in the different regions behind the dampers allowed the choose the most optimal variants of damper's plates with teeth and arcs on the trailing and leading edges for experimental analysis in reverberation rooms.
- The serrated and arced edges of the damper's plates allow the most efficient flow of air and are more uniform than for plat without the modifications.
- The serrated and arced edges of the damper's plate contribute to the obtained lower values of pressure drop.
- The experimental analysis of airflow across the damper's plate opened at  $45^\circ$  angle showed that the coefficient  $CD$  and loss coefficient is the lowest for variants 5 and 7.
- The experimental analysis of noise reduction and  $L_{wA}$  of the studied damper's plate showed that variant 5 the most reduces the noise in comparison to the "base" unit.

## Additional information

The authors declare: no competing financial interests and that all material taken from other sources (including their own published works) is clearly cited and that appropriate permits are obtained.

## References

- R. Liu, J. Wen, M.S. Waring; Improving airflow measurement accuracy in VAV terminal units using low conditioners; Building and Environment 2014, 71, 81–94.
- C. E. Kiper; Desing, construction and performance evaluations of a constant air volume device for HVAC systems; MSc Thesis, Graduate School of Natural and Applied Sciences of Middle East Technical University, Ankara, Turkey, 2018.
- D. Dickerhoff, J. Stein; Stability and accuracy of VAV terminal units at low flows. Application Assessment Report; Pacific Gas and Electric Company, San Carlos, USA, 2016.
- American Society of Heating, Refrigerating and Air-Conditioning Engineers; Sound and Vibration Control; In: ASHRAE Handbook – HVAC Applications (SI); American Society of Heating, Refrigerating and Air-Conditioning Engineers: Atlanta, USA, 2011.
- American Society of Heating, Refrigerating and Air-Conditioning Engineers; ASHRAE Handbook – HVAC Applications (SI); American Society of Heating, Refrigerating and Air-Conditioning Engineers: Atlanta, USA, 2007.
- European Parliament and the Council; Directive on the energy performance of buildings; European Parliament and the Council: Brussels, Belgium, 2010.

7. European Parliament and the Council; Ecodesign Directive 1253/2014; European Parliament and the Council: Brussels, Belgium, 2014.
8. ISO 5135:2020 Acoustics – Determination of sound power levels of noise from air-terminal devices, air-terminal units, dampers and valves by measurement in a reverberation test room.
9. Comsol – Software for Multiphysics Simulation
10. J. Pfitzner; Poiseuille and his law; *Anaesthesia* 1976, 31(2), 273–275. DOI: 10.1111/j.1365-2044.1976.tb11804.x
11. PN EN ISO 1751 Ventilation for buildings – air terminal devices – aerodynamic testing of damper and valves.
12. PN-EN ISO 3741:2011 Acoustics – Determination of sound power levels and sound energy levels of noise sources using sound pressure – Precision methods for reverberation test rooms.

© 2022 by the Authors. Licensee Poznan University of Technology (Poznan, Poland). This article is an open access article distributed under the terms and conditions of the Creative Commons Attribution (CC BY) license (<http://creativecommons.org/licenses/by/4.0/>).